

DOMAIN-INVARIANT MIXED-DOMAIN SEMI-SUPERVISED MEDICAL IMAGE SEGMENTATION WITH CLUSTERED MAXIMUM MEAN DISCREPANCY ALIGNMENT

Ba-Thinh Lam⁵ Thanh-Huy Nguyen¹ Hoang-Thien Nguyen^{1,2} Quang-Khai Bui-Tran^{2,3}
 Nguyen Lan Vi Vu¹ Phat K. Huynh² Ulas Bagci⁴ Min Xu^{1*}

¹Carnegie Mellon University, PA, USA

²PASSIO Lab, North Carolina A&T State University, NC, USA

³Ho Chi Minh University of Science, Vietnam

⁴Northwestern University, IL, USA

⁵University of North Carolina at Charlotte, NC, USA

ABSTRACT

Deep learning has shown remarkable progress in medical image semantic segmentation, yet its success heavily depends on large-scale expert annotations and consistent data distributions. In practice, annotations are scarce and images are collected from multiple scanners or centers, leading to mixed-domain settings with unknown domain labels and severe domain gaps. Existing semi-supervised or domain adaptation approaches typically assume either a single domain shift or access to explicit domain indices, which rarely hold in real-world deployment. In this paper, we propose a domain-invariant mixed-domain semi-supervised segmentation framework that jointly enhances data diversity and mitigates domain bias. A **Copy-Paste Mechanism (CPM)** augments the training set by transferring informative regions across domains, while a **Cluster Maximum Mean Discrepancy (CMMD)** block clusters unlabeled features and aligns them with labeled anchors via an MMD objective, encouraging domain-invariant representations. Integrated within a teacher–student framework, our method achieves robust and precise segmentation even with very few labeled examples and multiple unknown domain discrepancies. Experiments on Fundus and M&Ms benchmarks demonstrate that our approach consistently surpasses semi-supervised and domain adaptation methods, establishing a potential solution for mixed-domain semi-supervised medical image segmentation.

Index Terms— Semi-supervised learning, Domain Adaptation, Medical Image Segmentation

1. INTRODUCTION

Medical image segmentation is a potential task for computer-aided diagnosis, yet building reliable models often requires a large quantity of expert annotations. In practice, collecting

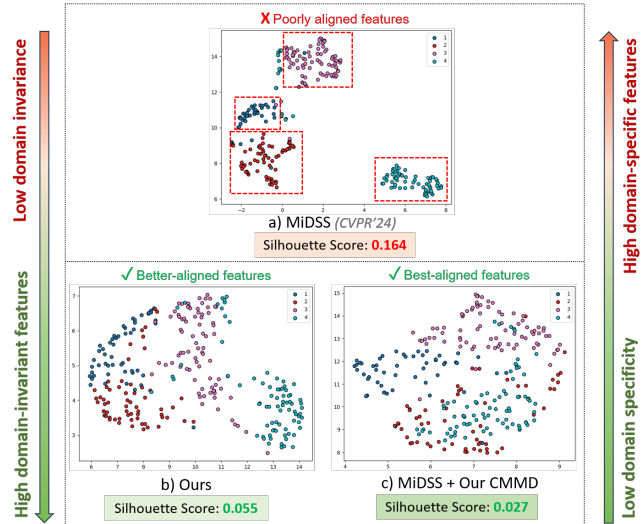


Fig. 1. Feature visualizations of the student encoder’s last layer on the Fundus dataset using UMAP. Domains are shown in different colors, and the model was trained with labeled samples from Domain 4. Silhouette Score assesses cluster quality, with higher scores indicating more separated clusters.

such labels is expensive and time-consuming, and the problem becomes even more challenging when data originate from multiple sources, scanners, or clinical centers. Models trained with a few labeled examples tend to overfit, while standard semi-supervised learning (SSL) [1, 2, 3, 4, 5, 6, 7] or domain adaptation (DA) [8, 9, 10, 11, 12] approaches frequently assume either a single target distribution or access to explicit domain labels, which rarely hold in real-world deployments.

Recent studies have begun to address this setting, often referred to as *mixed-domain semi-supervised segmentation*. Methods such as MiDSS [13] construct intermediate domains to bridge distribution gaps, showing encouraging results on benchmarks like Fundus [14] and M&Ms [15]. However,

* Corresponding Author: mxu1@cs.cmu.edu

this approach still does not solve the domain discrepancies thoroughly. Indeed, we investigate this by visualizing feature representations from pretrained models on Fundus. Fig. 1a shows learned features from MiDSS [13] cluster more separated by domains with a high Silhouette Score. This indicates that MiDSS produces domain-specific features instead of domain-invariant features. Plus, we can not directly apply common DA approaches to solve, due to the unknown domains and unprovided domain labels.

To address these challenges, we propose a simple yet effective framework that simultaneously enhances data diversity and mitigates domain bias explicitly in input and feature spaces. Specifically, we design a **Copy-Paste Mechanism (CPM)** to augment the training set by transferring informative regions across domains, thereby expanding the sample space under limited annotations. Also, a **Cluster Maximum Mean Discrepancy (CMMMD)** block is introduced to cluster unlabeled features and align them with labeled anchors through an MMD loss, promoting domain-invariant representations. By combining these modules within a teacher–student network, our method explicitly addresses multiple mixed-domain discrepancies and produces precise segmentation.

2. METHODOLOGY

2.1. Problem Definition

Let $\mathcal{S}_l = \{(x_i, y_i)\}_{i=1}^N$ be a small labeled set from domain D_j , and $\mathcal{S}_u = \{x_i\}_{i=1}^M$ a large unlabeled set from a mixture of domains $\{D_1, \dots, D_K\}$, with K unknown. The aim is to learn a segmentation model f_θ that generalizes across all domains using few labeled and many unlabeled samples.

This scenario differs from classical DA or SSL in two ways: (1) the unlabeled pool spans several hidden domains with no domain labels, and (2) K is not fixed or known, making standard DA inapplicable. Bridging D_j and $\{D_k\}$ thus requires discovering domain structure and mitigating discrepancies while preserving semantics.

As shown in Fig. 2, our framework tackles this by (i) enlarging the cross-domain training space via CPM, and (ii) learning domain-invariant features with CMMMD, which clusters unlabeled features and aligns them to labeled anchors through an MMD objective.

2.2. Copy-Paste Mechanism

To enrich the sample for model learning, we combine weak- and strong-augmented unlabeled examples x_u^w, x_u^s with labeled examples x_{lb} through Copy-Paste Mechanism (CPM):

$$x_{in}^w = (1 - \mathcal{M}) \odot x_u^w + \mathcal{M} \odot x_{lb}, \quad (1)$$

$$x_{out}^w = \mathcal{M} \odot x_u^w + (1 - \mathcal{M}) \odot x_{lb}, \quad (2)$$

$$x_{in}^s = (1 - \mathcal{M}) \odot x_u^s + \mathcal{M} \odot x_{lb}, \quad (3)$$

$$x_{out}^s = \mathcal{M} \odot x_u^s + (1 - \mathcal{M}) \odot x_{lb}, \quad (4)$$

where \mathcal{M} is a binary mask (1 indicates the region of interest). The models generate predictions for these mixed examples:

$$\hat{p}_{in}^w = T(x_{in}^w; \theta^T), \quad \hat{p}_{in}^s = S(x_{in}^s; \theta^S) \quad (5)$$

$$\hat{p}_{out}^w = T(x_{out}^w; \theta^T), \quad \hat{p}_{out}^s = S(x_{out}^s; \theta^S) \quad (6)$$

we use \hat{p}_{in}^w and \hat{p}_{out}^w as pseudo-labels to guide \hat{p}_{in}^s and \hat{p}_{out}^s by consistency losses \mathcal{L}_{in} and \mathcal{L}_{out} :

$$\mathcal{L}_{in} = Dice(\hat{p}_{in}^s, \hat{p}_{in}^w) + CE(\hat{p}_{in}^s, \hat{p}_{in}^w), \quad (7)$$

$$\mathcal{L}_{out} = Dice(\hat{p}_{out}^s, \hat{p}_{out}^w) + CE(\hat{p}_{out}^s, \hat{p}_{out}^w). \quad (8)$$

Finally, the CPM loss is computed as follows:

$$\mathcal{L}_{CPM} = \mathcal{L}_{in} + \mathcal{L}_{out}. \quad (9)$$

2.3. Cluster Maximum Mean Discrepancy Block

To handle inter-domain discrepancies, we propose the Cluster Maximum Mean Discrepancy Block (CMMMD), composed of a Clustering Module and a MMD-based Domain-Aware Module (Fig. 3). The Clustering Module estimates clusters from feature-space density, while the MMD-based Domain-Aware Module pulls them together by minimizing their Maximum Mean Discrepancy. CMMMD is applied to all encoder layers, ensuring domain signals are removed before final decoder predictions.

2.3.1. Clustering Module

Given the teacher model’s stability and generalization, we cluster unlabeled features x_u extracted from it. The teacher first processes weakly augmented inputs x_u^w to obtain features f_u^T at a chosen encoder layer:

$$f_u^T = E^T(x_u^w). \quad (10)$$

Because the number of domains is unknown, clustering is challenging. We address this by estimating clusters from feature-point density using Hierarchical Density-Based Spatial Clustering of Applications with Noise (HDBSCAN [16]):

$$(c_{u,1}, \dots, c_{u,Q}) = \text{HDBSCAN}(f_u^w, \text{minClusterSize}, \text{minSample}), \quad (11)$$

where $c_{u,i}$ is the centroid of cluster $C_{u,i}$ for unlabeled features, and Q is the predicted number of domains. As they update over epochs, these centroids are termed *pseudo-centroids*.

They are then used to assign pseudo-domain labels to weakly augmented features f_u^S extracted by the student encoder $E^S(\cdot; \theta_E^S)$:

$$f_u^S = E^S(x_u^w). \quad (12)$$

Distances to each pseudo-centroid are computed, and the label \hat{p}_d is set to the closest cluster:

$$d_i = \|f_u^S - c_{u,i}\|_2, \quad 1 \leq i \leq Q, \quad (13)$$

$$\hat{p}_d = \arg \min_{1 \leq i \leq Q} d_i. \quad (14)$$

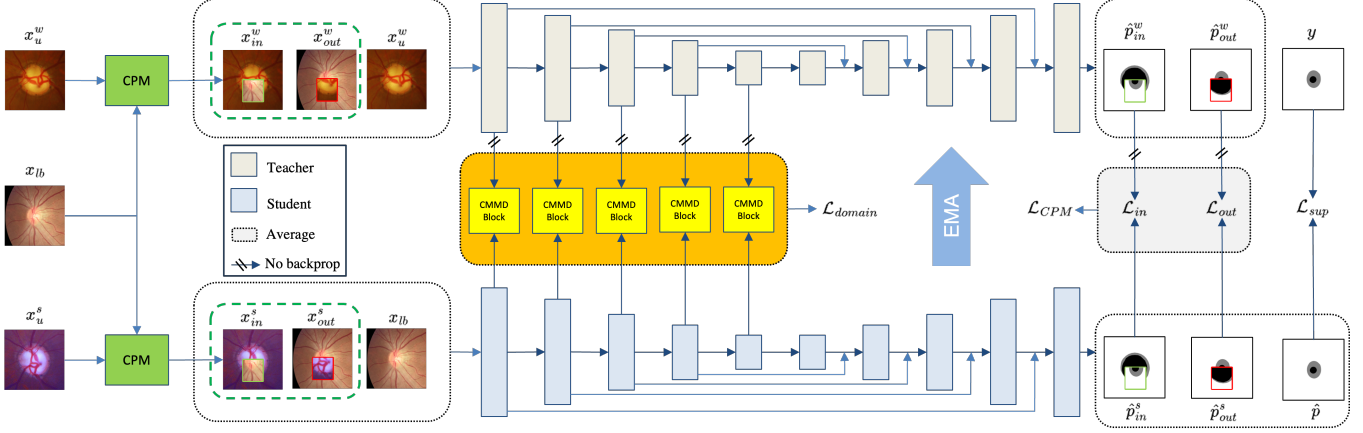


Fig. 2. Overall illustration of Our Framework.

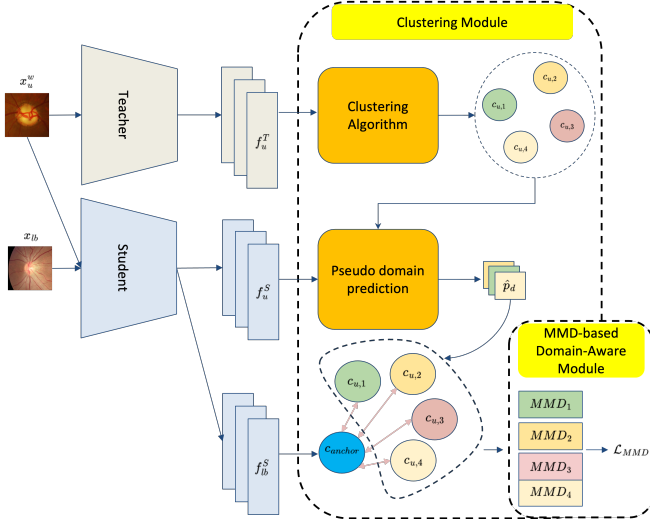


Fig. 3. Illustration of CMMMD Block.

2.3.2. MMD-based Domain-Aware Module

To reduce inter-domain gaps, we minimize Maximum Mean Discrepancy (MMD) between clusters. Computing MMD for all pairs is costly, so we pick a reliable anchor cluster and compute MMD w.r.t. it, pulling clusters together efficiently. Labeled features \$f_{lb}^S\$ act as the anchor \$C_{anchor}\$, since they are drawn i.i.d. from domain \$D_j\$. For cluster \$C_{u,i}\$:

$$\begin{aligned}
 MMD_i &= \text{MMD}^2(C_{u,i}, C_{anchor}) \\
 &= \frac{1}{m_i(m_i - 1)} \sum_p \sum_{q \neq p} k(\mathbf{c}_p^{(u,i)}, \mathbf{c}_q^{(u,i)}) \\
 &\quad - \frac{2}{m_i n} \sum_p \sum_q k(\mathbf{c}_p^{(u,i)}, \mathbf{c}_q^{(anchor)}) \\
 &\quad + \frac{1}{n(n-1)} \sum_p \sum_{q \neq p} k(\mathbf{c}_p^{(anchor)}, \mathbf{c}_q^{(anchor)}), \tag{15}
 \end{aligned}$$

where \$k(\mathbf{x}_i, \mathbf{x}_j) = \exp\left(-\frac{\|\mathbf{x}_i - \mathbf{x}_j\|^2}{2\sigma^2}\right)\$ is the gaussian kernel, \$m_i\$ is the number of features belonging to \$C_{u,i}\$, and \$n\$ is the number of features belonging to \$C_{anchor}\$. These MMD values are averaged to compute MMD loss \$\mathcal{L}_{MMD}\$, which is minimized to address the domain gaps:

$$\mathcal{L}_{MMD} = \frac{1}{Q} \sum_{i=1}^Q MMD_i. \tag{16}$$

2.3.3. Domain Loss

While CMMMD can handle domain gaps, the features extracted at layers of the decoder still remain domain signal due to skip connections among layers from the encoder and decoder. Plus, applying directly CMMMD for layers of the decoder may harm class predictions of the model, because these decoder features bring more information about class decisions than the domain information.

To address this issue, we apply CMMMD for all layers of the encoder to remove domain information from intermediate features of the encoder before transferring to the decoder through skip connections. In this way, we compute MMD loss \$\mathcal{L}_{MMD}^l\$ at the \$l\$th layer, respectively. Eventually, the Domain loss \$\mathcal{L}_{domain}\$ is computed as follows:

$$\mathcal{L}_{domain} = \frac{1}{L} \sum_{l=1}^L \mathcal{L}_{MMD}^l, \tag{17}$$

where \$L\$ is the number of encoder layers (\$L = 5\$, commonly).

2.4. Final Loss

The Domain loss is combined with the CPM loss and the Supervised loss to compute the total loss:

$$\mathcal{L}_{total} = \mathcal{L}_{sup} + w(\mathcal{L}_{CPM} + \mathcal{L}_{domain}), \tag{18}$$

where \$w\$ is a dynamic coefficient updated by an iteration-dependent Gaussian function, \$w = \exp(-5(1 - \frac{iter}{iter_{max}}))\$.

3. EXPERIMENTAL RESULTS

3.1. Datasets & Metrics

We evaluate on Fundus and M&Ms using Dice (DC), Jaccard (JC), Hausdorff distance (HD), and Average Surface Distance (ASD). Both teacher and student adopt UNet [17]. Training uses 30k and 60k iterations for Fundus and M&Ms, respectively. HDBSCAN is set with $minClusterSize=10$ and $minSample=5$. All runs are on A5000/RTX3090 GPUs.

3.2. Results

For fair comparison, we reproduced the results of MiDSS [13] for all experiments.

Fundus. With only 20 labeled images (Table 1), SSL baselines (UA-MT [4], CPS [5]) show modest gains, while FixMatch [2] and BCP [3] remain vulnerable to hidden domains. MiDSS mitigates but does not eliminate domain gaps. Our method, combining CPM and CMMD, enlarges the training space via mixed-domain patches and aligns features through an MMD loss, achieving a steady edge over MiDSS (DC $\approx 87\%$).

Table 1. Comparison of different methods on Fundus dataset. The number of labeled examples is 20. Higher is better for DC/JC, lower is better for HD/ASD. Best in **bold**, second-best underlined.

Method	DC \uparrow (Optic Cup / Disc)				Avg.	Avg.	Avg.	Avg.
	Domain 1	Domain 2	Domain 3	Domain 4				
U-Net	59.54 / 73.89	71.28 / 74.23	50.87 / 64.29	35.61 / 63.30	61.63	52.65	48.28	28.86
UA-MT	59.35 / 78.46	63.08 / 74.45	35.24 / 47.73	36.18 / 55.43	56.24	47.00	48.64	31.55
FDA	76.99 / 89.94	77.69 / 89.63	78.27 / 90.96	64.52 / 74.29	80.29	71.05	16.23	8.44
FixMatch	81.18 / 91.29	72.04 / 87.60	80.41 / 92.95	74.58 / 87.07	83.39	73.48	11.77	5.60
CPS	64.53 / 86.25	70.26 / 86.97	42.92 / 54.94	36.98 / 46.70	61.19	52.69	34.44	26.79
CoraNet	61.64 / 87.32	65.56 / 87.05	66.12 / 83.54	49.01 / 77.73	72.26	65.00	20.52	10.44
UDA-VAE++	55.01 / 80.76	68.87 / 85.94	63.23 / 84.92	68.42 / 80.89	73.51	61.40	17.60	9.86
BCP	71.65 / 91.10	77.19 / 92.00	72.63 / 90.77	77.67 / 91.42	83.05	73.66	11.05	5.80
CauSSL	63.38 / 80.60	67.52 / 80.72	49.53 / 63.88	39.43 / 49.43	61.81	51.80	41.25	23.94
MiDSS (reproduced)	82.17 / 95.35	77.56 / 90.55	82.23 / 92.89	83.34 / 91.22	86.91	78.12	8.24	3.95
Ours	81.23 / 94.84	78.39 / 89.26	83.37 / 92.84	84.09 / 91.92	86.99	78.22	8.25	3.96

M&Ms. Table 2 reports results on M&Ms with 20 labeled images. FixMatch and BCP perform well but leave scanner gaps. MiDSS improves via intermediate domains yet retains bias. Combining CPM and CMMD yields the best scores (DC ≈ 84.4 , JC ≈ 75).

3.3. Ablation & Analysis

We assess our method on Fundus using 20 labeled and the rest unlabeled images.

Efficiency of CPM and CMMD. Table 3 reports the effect of each component. The baseline is a UNet teacher–student with cross-entropy and weak-to-strong consistency. Adding CPM raises DC/JC by 3.83%/4.88%, confirming the benefit of mixed-domain augmentation. Integrating CMMD further lifts performance to DC 86.99% and JC 78.22%, highlighting its ability to reduce domain discrepancies.

Plug-in Property of CMMD. Table 4 shows that adding CMMD to MiDSS lifts DC/JC to 87.18%/78.45%, confirm-

Table 2. Comparison of different methods on M&Ms dataset. The number of labeled examples is 20. Higher is better for DC/JC, lower is better for HD/ASD. Best in **bold**, second-best underlined.

Method	DC \uparrow (UV / MYO / RV)				DC \uparrow	JC \uparrow	HD \downarrow	ASD \downarrow
	Vendor A	Vendor B	Vendor C	Vendor D				
U-Net	57.29 / 37.85 / 34.65	73.44 / 64.20 / 53.58	55.83 / 48.47 / 44.84	63.85 / 52.25 / 49.85	53.01	44.30	38.07	22.88
UA-MT	38.02 / 25.55 / 14.94	61.85 / 54.27 / 47.33	43.13 / 35.06 / 28.82	41.89 / 38.25 / 26.41	37.90	29.14	72.35	40.84
FDA	61.60 / 54.25 / 47.33	80.10 / 72.27 / 60.56	77.23 / 70.23 / 63.53	62.26	53.21	29.33	19.10	
FixMatch	87.26 / 77.38 / 77.14	81.06 / 82.78 / 79.07	87.84 / 80.07 / 78.03	87.06 / 81.75 / 81.84	87.99	62.21	3.51	
CPS	46.40 / 29.01 / 16.70	71.48 / 63.08 / 49.39	44.38 / 39.43 / 32.42	47.71 / 40.75 / 29.75	42.54	33.82	58.30	34.94
CoraNet	65.70 / 27.79 / 22.16	63.32 / 48.63 / 46.56	64.89 / 48.59 / 45.30	50.33	40.54	19.22		
UDA-VAE++	51.14 / 36.20 / 12.99	71.95 / 53.16 / 36.68	57.88 / 41.64 / 30.19	31.71 / 27.32 / 20.48	39.28	28.82	53.90	24.94
BCP	85.91 / 73.82 / 78.08	85.66 / 74.85 / 76.04	61.61 / 54.05 / 51.87	76.57 / 62.22 / 79.16	71.65	62.67	30.91	18.22
CauSSL	40.20 / 21.93 / 10.46	50.99 / 42.66 / 31.94	41.05 / 34.00 / 29.95	53.78 / 37.92 / 30.44	35.44	26.73	72.90	37.99
MiDSS (reproduced)	89.66 / 80.44 / 80.93	89.86 / 84.27 / 85.93	89.75 / 79.98 / 76.77	89.01 / 81.54 / 83.35	84.25	75.20	5.08	2.54
Ours	90.27 / 80.53 / 80.97	90.17 / 84.46 / 85.77	90.12 / 79.70 / 75.56	89.77 / 81.72 / 83.53	84.35	75.33	5.21	2.57

Table 3. Ablation study for components of our framework on Fundus dataset.

Ablation	Component	DC \uparrow				Avg.	Avg.		
		CPM	CMMD	Domain 1	Domain 2	Domain 3	Domain 4	DC \uparrow	JC \uparrow
Baseline				74.96 / 93.50	71.08 / 85.72	77.45 / 89.10	81.32 / 91.36	83.06	73.19
1	✓			82.39 / 95.08	77.78 / 90.24	82.15 / 92.81	84.33 / 90.80	86.89	78.07
2	✓	✓		81.23 / 94.84	78.39 / 89.26	83.37 / 92.84	84.09 / 91.92	86.99	78.22

Table 4. Comparison of MiDSS before and after integrating our CMMD on Fundus.

Method	DC \uparrow				Avg.	Avg.
	Domain 1	Domain 2	Domain 3	Domain 4		
MiDSS (reproduced)	82.17 / 95.35	77.56 / 90.55	82.23 / 92.89	83.34 / 91.22	86.91	78.12
MiDSS + Our CMMD	83.21 / 95.63	78.36 / 91.48	82.02 / 92.71	83.30 / 90.75	87.18	78.45

ing its ability to reduce domain gaps. Since CMMD acts in the feature space, it can be easily integrated into other frameworks without extra parameters.

Domain gap alleviation by CMMD. Fig. 1 shows UMAP embeddings from the 5th encoder layer. MiDSS features form separate clusters (e.g., domain 4 is most isolated), revealing domain gaps. Adding CMMD yields more mixed representations, indicating reduced domain-specific variation and consistent learning of domain-invariant features.

4. CONCLUSION

We introduced a domain-invariant framework for mixed-domain semi-supervised medical image segmentation. By combining the Copy-Paste Mechanism (CPM) with the Cluster Maximum Mean Discrepancy (CMMD) block, our method enriches cross-domain training data and aligns unlabeled features with labeled anchors, effectively mitigating domain gaps explicitly. Integrated into a teacher–student network, it achieves consistent improvements on Fundus and M&Ms benchmarks, surpassing several semi-supervised learning and domain adaptation methods. Future work will explore extending CMMD to more complicated architectures and additional modalities, further advancing robust segmentation under limited annotations and multiple hidden distribution mismatches.

5. REFERENCES

[1] Yinghuan Shi, Jian Zhang, Tong Ling, Jiwen Lu, Yefeng Zheng, Qian Yu, Lei Qi, and Yang Gao, “Inconsistency-aware uncertainty estimation for semi-supervised medical image segmentation,” *IEEE transactions on medical imaging*, vol. 41, no. 3, pp. 608–620, 2021.

[2] Kihyuk Sohn, David Berthelot, Nicholas Carlini, Zizhao Zhang, Han Zhang, Colin A Raffel, Ekin Dogus Cubuk, Alexey Kurakin, and Chun-Liang Li, “Fixmatch: Simplifying semi-supervised learning with consistency and confidence,” *Advances in neural information processing systems*, vol. 33, pp. 596–608, 2020.

[3] Yunhao Bai, Duowen Chen, Qingli Li, Wei Shen, and Yan Wang, “Bidirectional copy-paste for semi-supervised medical image segmentation,” in *Proceedings of the IEEE/CVF conference on computer vision and pattern recognition*, 2023, pp. 11514–11524.

[4] Lequan Yu, Shujun Wang, Xiaomeng Li, Chi-Wing Fu, and Pheng-Ann Heng, “Uncertainty-aware self-ensembling model for semi-supervised 3d left atrium segmentation,” in *International conference on medical image computing and computer-assisted intervention*. Springer, 2019, pp. 605–613.

[5] Xiaokang Chen, Yuhui Yuan, Gang Zeng, and Jingdong Wang, “Semi-supervised semantic segmentation with cross pseudo supervision,” in *Proceedings of the IEEE/CVF conference on computer vision and pattern recognition*, 2021, pp. 2613–2622.

[6] Thanh-Huy Nguyen, Nguyen Lan Vi Vu, Hoang-Thien Nguyen, Quang-Vinh Dinh, Xingjian Li, and Min Xu, “Semi-supervised histopathology image segmentation with feature diversified collaborative learning,” in *Proceedings of The First AAAI Bridge Program on AI for Medicine and Healthcare*. 25 Feb 2025, vol. 281 of *Proceedings of Machine Learning Research*, pp. 165–172, PMLR.

[7] Juzheng Miao, Cheng Chen, Furui Liu, Hao Wei, and Pheng-Ann Heng, “Caussl: Causality-inspired semi-supervised learning for medical image segmentation,” in *Proceedings of the IEEE/CVF International Conference on Computer Vision (ICCV)*, October 2023, pp. 21426–21437.

[8] Hao Guan and Mingxia Liu, “Domain adaptation for medical image analysis: A survey,” *IEEE Transactions on Biomedical Engineering*, vol. 69, no. 3, pp. 1173–1185, 2022.

[9] Yanchao Yang and Stefano Soatto, “Fda: Fourier domain adaptation for semantic segmentation,” in *2020 IEEE/CVF Conference on Computer Vision and Pattern Recognition (CVPR)*, 2020, pp. 4084–4094.

[10] Changjie Lu, Shen Zheng, and Gaurav Gupta, “Unsupervised domain adaptation for cardiac segmentation: Towards structure mutual information maximization,” in *Proceedings of the IEEE/CVF conference on computer vision and pattern recognition*, 2022, pp. 2588–2597.

[11] Eric Tzeng, Judy Hoffman, Kate Saenko, and Trevor Darrell, “Adversarial discriminative domain adaptation,” in *Proceedings of the IEEE conference on computer vision and pattern recognition*, 2017, pp. 7167–7176.

[12] Kuniaki Saito, Donghyun Kim, Stan Sclaroff, Trevor Darrell, and Kate Saenko, “Semi-supervised domain adaptation via minimax entropy,” in *Proceedings of the IEEE/CVF international conference on computer vision*, 2019, pp. 8050–8058.

[13] Qinghe Ma, Jian Zhang, Lei Qi, Qian Yu, Yinghuan Shi, and Yang Gao, “Constructing and exploring intermediate domains in mixed domain semi-supervised medical image segmentation,” in *Proceedings of the IEEE/CVF conference on computer vision and pattern recognition*, 2024, pp. 11642–11651.

[14] Shujun Wang, Lequan Yu, Kang Li, Xin Yang, Chi-Wing Fu, and Pheng-Ann Heng, “Dofe: Domain-oriented feature embedding for generalizable fundus image segmentation on unseen datasets,” *IEEE Transactions on Medical Imaging*, vol. 39, no. 12, pp. 4237–4248, 2020.

[15] Victor M Campello, Polyxeni Gkontra, Cristian Izquierdo, Carlos Martin-Isla, Alireza Sojoudi, Peter M Full, Klaus Maier-Hein, Yao Zhang, Zhiqiang He, Jun Ma, et al., “Multi-centre, multi-vendor and multi-disease cardiac segmentation: the m&ms challenge,” *IEEE Transactions on Medical Imaging*, vol. 40, no. 12, pp. 3543–3554, 2021.

[16] Ricardo JGB Campello, Davoud Moulavi, and Jörg Sander, “Density-based clustering based on hierarchical density estimates,” in *Pacific-Asia conference on knowledge discovery and data mining*. Springer, 2013, pp. 160–172.

[17] Olaf Ronneberger, Philipp Fischer, and Thomas Brox, “U-net: Convolutional networks for biomedical image segmentation,” in *International Conference on Medical image computing and computer-assisted intervention*. Springer, 2015, pp. 234–241.